07

The nature of terahertz radiation in magnetic nanojunctions when current flows through them

© S.G. Chigarev, E.A. Vilkov, O.A. Byshevski-Konopko, A.I. Panas, L.A. Fomin, I.V. Malikov

- ¹ Fryazino Branch, Kotel'nikov Institute of Radio Engineering and Electronics, Russian Academy of Sciences,
- 141190 Fryazino, Moscow oblast, Russia
- ² State Scientific-Production Enterprise "Istok"
- 141190 Fryazino, Moscow oblast, Russia
- ³ Institute of Microelectronics Technology and High Purity Materials, Russian Academy of Sciences,

142432 Chernogolovka, Moscow oblast, Russia

e-mail: chig50@mail.ru

Received January 22, 2024 Revised March 13, 2025 Accepted March 24, 2025

The modes of operation of a spin-injected THz-emitter using a rod-film structure in the region of starting current values (current density) have been investigated. For Fe_3O_4 and Fe films, two mechanisms of THz-emission emergence have been experimentally established. One of them is related to the change in the energy of the sd-exchange interaction during the transition of the magnetic layer interface by spin-polarized current, when a part of electrons decreases its energy without spin flip, and the other is determined by interband transitions with spin flip at high values of current density. The theoretical substantiation of the observed two mechanisms of THz-radiation excitation is carried out.

Keywords: spin, magnetic transition, spin polarization, sd-exchange interaction, THz-radiation.

DOI: 10.61011/TP.2025.07.61459.16-24

Introduction

In recent years, the "terahertz range" (THz) attracts increasingly greater attention due to its unique features. Thus, terahertz radiation is not an ionizing one, thereby unaffecting bioobjects and can be successfully applied in medicine and biology. These frequencies can be used in safety systems, for example, to detect narcotics and explosives as well as to identify hidden items dangerous to the public. Wide frequency bands of this range enable creating super-fast information-communication systems, while wavelengths of these frequencies, that are commeasurable with typical sizes of the microcosm, make them promising for solving various materials science problems [1]. However, absence of compact, publicly available, reliable and simple-to-use sources and receivers of this range hinders its wide application. The commercially available THzsources available today, such as backward-wave tubes, freeelectron lasers, gas lasers and gas-discharge THz-sources as well as quantum-cascade lasers are far from meeting the requirements of simplicity and reliability. That is why it is still relevant to search for fundamentally new methods of generation and registration of terahertz radiation.

One of the promising areas in creation of THz-range hardware can be a new field of electronics known as spintronics. It studies and uses effects observed during electron-wave interaction with taking into account not only the electron charge, but its own magnetic moment (spin). Thus, in recent 10 to 15 years, mainly in Russia, there is a new developing field of studying principles of formation

of THZ signals (within the frequency range $7-30\,\mathrm{THz}$) in magnetic junctions that are made up of contacting layers of nanometer-thick ferromagnetics or antiferromagnetics while injecting into them spins by means of high-density current $(10^5-10^7\,\mathrm{A/cm^2})$ [2]. These studies have begun with theoretical papers [3,4] which predicted THz-radiation excitation during spin injection by current in the said structures and explained the effect of formation of spin-injection (dynamic) radiation. Of particular note is an original idea of interaction of electron spins with the electromagnetic radiation via sd-exchange as proposed in the paper [3]. According to estimates, such an interaction channel is by orders of magnitude more efficient than standard multi-pole channels. The subsequent experimental papers [5–8] confirmed the theoretical predictions.

Nevertheless, despite certain successes in studying the processes of formation of spin-injected THz-radiation, there is still a number of unresolved issues. Thus, the papers [9–11] note a complex nature of power variation of dynamic radiation when varying injection current in the region of radiation emergence. Deeper understanding of this process required additional elaboration of the published results as well as carrying out additional measurements. These measurements and the research as a whole are aimed at identifying various conditions of formation of the electromagnetic radiation during spin injection by current in the magnetic junctions. And in all the studies, newly detected effects are explained based on available theoretical notions about THz-radiation generation during spin injection by current in the magnetic nanojunctions.

1. Experimental results

The THz-radiation excitation modes in the various magnetic nanojunctions have been studied using an emitter based on a rod-film contact that is shown schematically on Fig. 1. The rod was an iron needle sharpened at one of the ends to the diameter $10-50\,\mu\mathrm{m}$. The emitter used thin-film samples prepared at IPTM RAS (city of Chernogolovka), which consisted of Fe films of the thickness of 30 and 60 nm and Fe₃O₄ films of the thickness of 30 nm grown on the sapphire *R*-plane by the ultrahigh vacuum pulsed laser vaporization method. The rod is magnetized up to saturation along its axis, while film magnetization is oriented in a normal to its plane up to saturation so as it is opposite to rod magnetization (antiparallel).

The device was powered by a DC source with smooth adjustment of stabilized voltage. The radiation generated in the rod-film contact point was focused by a high-resistivity silicon meniscus lens. The signal was recorded by "Tydex" Golay cell. Analog values for further treatment were digitized using AKTAKOM ASK-3117 storage oscilloscope. The measurements were performed within the current region from 0 to 700 mA with smooth variation of voltage to the emitter, thereby detecting a fine structure of the process of formation of THz-radiation.

Unlike previous articles, which used current during result processing as a parameter, the present paper deals with a current density. This may be attributed to the fact that, first, a basic parameter of the theoretical papers is the current density [12–14] and, secondly, as demonstrated in [15], the current density value at which the radiation emerges, is determined by a film material and is virtually

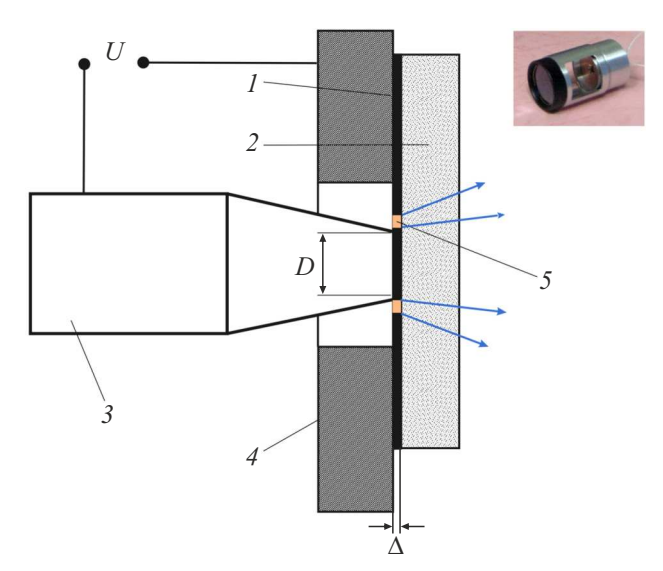


Figure 1. Diagram of the rod-film emitter: I — magnetic film, 2 — sample substrate, 3 — current-conducting magnetic rod, 4 — current collector contact, 5 — ring-form operating region, U — power supply potential, D — rod tip diameter, Δ — the thickness of the magnetic film. The arrows diverging out of the operating regions — THz-radiation. In the upper right corner — a picture of the actual mockup emitter with a focusing lens.

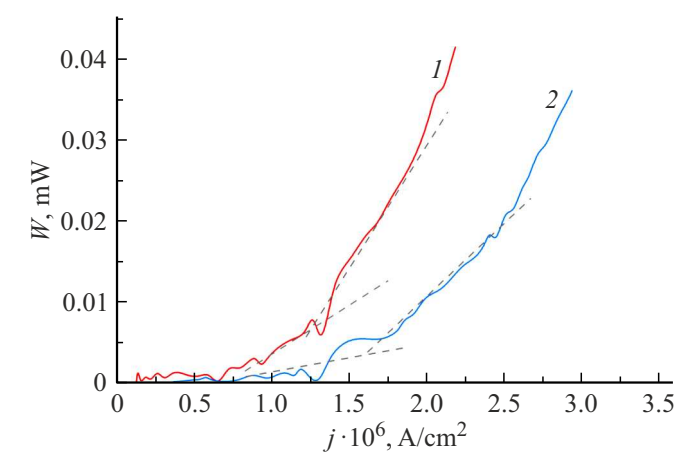


Figure 2. Dependence of radiation power W on the current density j for the spin-injected emitter with the rod-film structure when using the Fe iron film with the various film thickness Δ in it: the curve I — 30 nm, the curve 2 — 60 nm. Dashed straight lines — linear approximations of some curve sections.

independent of its thickness and structure. As shown below, it additionally contributes to reasoning when explaining observed effects and comparing operation modes of the emitters using different films which are made, inter alia, of the same material.

Fig. 2 shows the results of measurement of radiation power depending on variation of the density of current penetrating the Fe rod-Fe film structure for the two different film thicknesses. It is clear from Fig. 2 that at the initial portion of the curves emergence of radiation smoothly exceeding the zero level is observed for both the films with the current density value $j \sim 0.9 \cdot 10^6 \,\mathrm{A/cm^2}$ (starting With another current density value current density). $j \sim 1.3 \cdot 10^6 \,\mathrm{A/cm^2}$, which is the same for both the films, there is observed sharp increase of power in the current density band $\Delta j \sim 0.1 \cdot 10^6 \, \text{A/cm}^2$ with subsequent change of its increase slope. The increase slope is approximated with the dashed lines. In accordance with the paper [12– 15], this curve behavior may indicate emergence of an additional radiation source in the studied structure with $j \sim 1.3 \cdot 10^6 \,\mathrm{A/cm^2}$, wherein this source is of another nature different from the initial portion within the current density range $i \sim (0.9-1.3) \cdot 10^6 \,\mathrm{A/cm^2}$. The equality of the current densities for both the iron films both when smoothly exceeding the zero power level and with sharp increase of the power in the now operating emitter indicates a spin-injected mechanism of generation excitation in both the cases.

The different ratio of the starting values of the current densities is observed when using the emitters with the films made of different materials. As an example, Fig. 3 compares the results obtained for the two "rod–film" structures using the films of the same thickness of 30 nm Fe (spin polarization $P\sim0.4$) and Fe₃O₄ ($P\sim1$). In both the structures the rod is made of Fe. It is clear

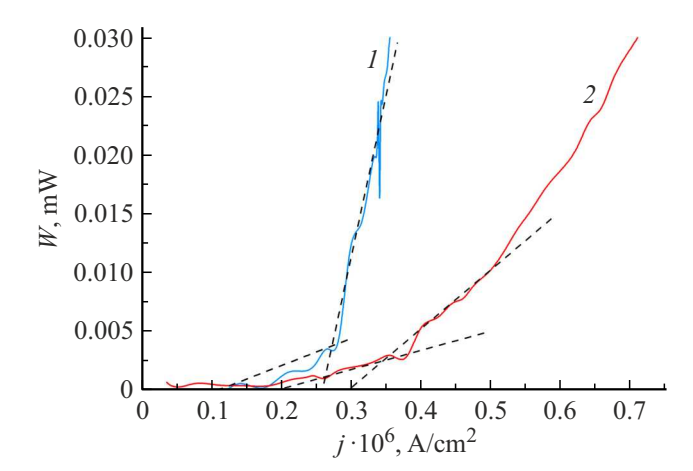


Figure 3. Dependence of the radiation power W on the current density j for the two magnetic junctions: the curve I — Fe₃O₄/Fe, the curve 2 — Fe/Fe. In both the cases the film thickness is 30 nm. Dashed straight lines — linear approximations of some curve sections.

from the figure that for the different ferromagnetics the electromagnetic oscillations are excited at the different current densities, which does not contradict to [12–15]. However, a qualitatively identical pattern is observed for both the structures. Thus, for both the cases, when exceeding a certain starting value of the current density for the Fe₃O₄ film — $j \sim 0.45 \cdot 10^6$ A/cm², and for the Fe film — $j \sim 0.7 \cdot 10^6 \,\text{A/cm}^2$ there is emergence of radiation with subsequent smooth increase of the power. As the current density increases, both the cases exhibit sharp variation of power for the Fe₃O₄ film at $j \sim 1 \cdot 10^6$ A/cm² and for the Fe film at $j \sim 1.3 \cdot 10^6 \,\mathrm{A/cm^2}$, after which the power increase slope varies with growth of the current density. It is clear that for the structure with the Fe₃O₄ film, in which a value of the equilibrium spin polarization is close to unity, the radiation power increases more sharply with increase of the current density than for the structure with the Fe film.

The identity of the processes of formation of radiation in these structures may be additionally confirmed by a "dip" of the power before its jump. For explanation of it, let us use results of [8–10], according to which interband transitions can be both direct ones without the third particle and indirect ones. The latter are relation to absorption of the third particle (phonon). Thus, the "dip" can be explained by some decrease of the emitter temperature related to absorption of the phonons in indirect quantum transitions, which finally results in some decrease of the registered signal level. With increase of the current density, the radiation power increases and influence of "cooling" of the emitter on the level of the registered signal becomes insignificant.

The above results show a complex picture of THz-radiation formation in the magnetic nanojunctions during spin injection by current: smooth increase of the power when exceeding some starting value of the current density

and sharp variation of the power when reaching the higher current density in the now operating emitter.

2. Substantiation of the results obtained

In accordance with common notions about operation of the spin-injected emitters formed by at least two contacting magnetic nanolayers with substantially different magnetic characteristics (for example, orientation of magnetization M_1, M_2), the current penetrating the junction is polarized by the electron spin (the spin is polarized) in one of the layers which is called an injector, i.e. the spins of conductivity electrons are oriented parallel or antiparallel to injector magnetization [16]. The spin-polarized current of the density j, which is injected into the second operating layer, disturbs the equilibrium spin state P_2 in it. In accordance with the paper [17], the non-equilibrium spin polarization is calculated using the following formula when $j/j_D \gg 1$:

$$P(x) = P_2 + \frac{P_1 \cos \varphi - P_2}{j + j_D} j \exp(-x/l), \qquad (1)$$

where x — the distance from the boundary of the materials, the angle between the magnetizations M_1 and M_2 , $l = \sqrt{D\tau} \sim 3 \cdot 10^{-6}$ cm the spin relaxation length, D — the diffusion constant, τ — the spin relaxation time, $j_D = enD/l = enl/\tau$ — the electron diffusion current density, n — the concentration of electrons in the metal, P_1, P_2 — the equilibrium spin polarizations in the first and the second ferromagnetic, e — the electron charge. With substitution of typical estimates of the parameters $n \sim 10^{22} \, \mathrm{cm}^{-3}$ and $\tau \sim 3 \cdot 10^{-13} \, \mathrm{s}$, we obtain $j_D \sim 1.6 \cdot 10^{10} \, \mathrm{A/cm^2}$. Since the maximum currents in the magnetic junctions used in the experiment usually are by an order of magnitude less than the obtained value, it may be assumed that the condition $j/j_D \gg 1$ is well met.

Thus, there is deviation $\Delta P = P - P_2$ of spin polarization from the equilibrium one P_2 . At the same time, in the operating layer, at the distance of spin relaxation from the layer interface, the energy subbands with the opposite spin that are originally balanced in the injector with the same Fermi level $e_{\rm F0}$, as the electron spin state varies more slowly than variation of its energy and momentum, are expanded by energy to form in each of the subbands the Fermin quasilevels spaced apart above $e_{\rm F+}$ and below $e_{\rm F-}$ by the energy in relation to their equilibrium levels $e_{\rm 0F+,-}$ [17]. The diagram for formation of the Fermi quasi-levels is shown on Fig. 4.

$$\varepsilon_{F+} - \varepsilon_{0F+} = \frac{\hbar^2}{2m} (3\pi^2 n)^{2/3} \times \left(\left(\frac{1 - P_2 - \Delta P}{2} \right)^{2/3} - \left(\frac{1 - P_2}{2} \right)^{2/3} \right), \quad (2)$$

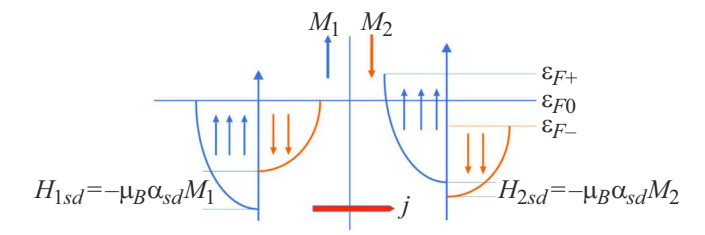


Figure 4. Diagram of formation of the Fermi quasi-levels without taking into account influence of power supply voltage. The spin-polarized current of magnetization M_1 in the "left" layer of the magnetic junction is distributed along spin-energy subbands, in which the electrons are in a balanced state having the same Fermi level $e_{\rm F0}$. Going over to the "right" layer with magnetization M_2 , occupation of the spin-energy subbands is still the same with variation of their energy. The subbands are expanded by energy. The spin equilibrium is disturbed, thereby resulting in formation of the Fermi quasi-levels $e_{\rm F+}$ and $E_{\rm F-}$.

$$\varepsilon_{F-} - \varepsilon_{0F-} = \frac{\hbar^2}{2m} (3\pi^2 n)^{2/3} \times \left(\left(\frac{1 + P_2}{2} \right)^{2/3} - \left(\frac{1 + P_2 + \Delta P}{2} \right)^{2/3} \right), \quad (3)$$

where n — the electron concentration in the metal. Thus, one of the subbands with $e_{\rm F+}$ exhibits spin-non-equilibrium, energy-excited ("hot") electrons in the unstable equilibrium, while the second subband with $e_{\rm F-}$ exhibits vacant energy levels. This situation allows the "hot" electrons under impact of external radiation making transitions into another energy subband with spin flip with giving away a part of its energy as a radiation quantum, i.e. making radiative transitions.

Without taking into account mechanisms of relaxation and interaction with the electromagnetic field, the electron energy can be written as a Hamiltonian [12]:

$$\hat{H}(\hat{\mathbf{p}}) = \hat{\sigma}_0 \frac{\hat{\mathbf{p}}^2}{2m} - \hat{\boldsymbol{\sigma}} \mathbf{I}(\mathbf{p}), \tag{4}$$

where m — the effective mass of the electron, $\hat{\mathbf{p}}$ — the operator of generalized canonic momentum [18], $\hat{\boldsymbol{\sigma}}$ — the Pauli matrix vector, $\hat{\sigma}_0$ — the unity matrix sized as 2×2 , $|\mu_B \alpha_{sd} \mathbf{M}_2| = I$ — the exchange energy, μ_B — the Bohr magneton, $\alpha_{sd} \sim 2 \cdot 10^4$ — the constant of sd-exchange, \mathbf{M}_2 — magnetization of the operating region.

In the presence of the electromagnetic field with the vector potential $\mathbf{A} = \mathbf{A}_0 \exp(i\omega t + \mathbf{k}\mathbf{r})$, where ω — the frequency of the external signal, the electron momentum operator shall be replaced as per [18] by $(\mathbf{p} - \frac{e}{c}\mathbf{A})$. Taking into account the above said, (4) can be rewritten as

$$\hat{H} = \hat{\sigma}_0 \varepsilon \left(\mathbf{p} - \frac{e}{c} \mathbf{A} \right) - \hat{\boldsymbol{\sigma}} \mathbf{I} \left(\mathbf{p} - \frac{e}{c} \mathbf{A} \right). \tag{5}$$

Here ε — the kinetic energy of the electron, e — the electron charge, c — the velocity speed, $\mu_B \alpha_{sd} \mathbf{M}_2 = \mathbf{I}$.

Following [12] and expanding (5) into a series in powers of the small parameter e/c $|\mathbf{A}|$, we obtain the following

taking into account linear terms of expansion

$$\mathbf{I}\Big(\hat{\mathbf{p}} - \frac{e}{c}\,\mathbf{A}\Big) \approx \mathbf{I}(\mathbf{p}) - \frac{e}{2c} \bigg(\frac{\partial \mathbf{I}}{\partial \hat{\mathbf{p}}}\,\mathbf{A} + \mathbf{A}\,\frac{\partial \mathbf{I}}{\partial \hat{\mathbf{p}}}\bigg),$$

$$\varepsilon \left(\hat{\mathbf{p}} - \frac{e}{c}\mathbf{A}\right) \approx \frac{\mathbf{p}^2}{2m} - \frac{e}{2mc}(\hat{\mathbf{p}}\mathbf{A} + \mathbf{A}\hat{\mathbf{p}}).$$
 (6)

Let us rewrite (5) taking into account (6) as

$$H = \frac{p^2}{2m} \mp I + \frac{e}{2c} \left\{ \frac{\partial \mathbf{I}}{\partial \mathbf{p}} \mathbf{A} + \mathbf{A} \frac{\partial \mathbf{I}}{\partial \mathbf{p}} \right\}. \tag{7}$$

At the same time we neglect the operator

$$\hat{H} = \hat{\sigma}_0 \, \frac{e}{mc} \, \mathbf{A} \hat{\mathbf{p}},$$

since its action does not cause spin flip. It is clear from (7) that the formation of the spin-injected radiation in the magnetic junction can be described by a relationship consisting in two parts: one part includes the first two terms (7), which describe the electron energy with certain orientation of the spin in relation to magnetization of the operating layer, while the other part - (7) describes disturbance by external electromagnetic radiation. The last summand in (7) having off-diagonal elements will be responsible for the electron spin flip mechanism in the interband transitions. Using the last summand in (7) as disturbance, the paper [19] has calculated a number of the transitions per unit time:

$$R_{st} = \frac{6\pi^2 e^2 \mu}{n_0^2 \omega} \frac{(n_{\uparrow} - n_{\downarrow})}{\hbar \nu_s} N_P \left(\frac{\partial I}{\partial p_i}\right)^2 (\cos^2 \varphi), \quad (8)$$

where μ and n_0 — permeability and refractive index of the metal ferromagnetic, respectively, n_{\uparrow} and n_{\downarrow} — the density of electron with the spin up and down, N_p — the density of photons of the external magnetic field, the frequency of spin relaxation $\nu_s \approx 10^{12}\,\mathrm{Hz}$.

The power can be calculated by multiplying the number of quantum transitions per unit time (see (8)) by the quantum energy, which can be found by the formula

$$W = \hbar \omega R_{st}$$
.

Let us take experimental data: the spin relaxation frequency $\nu_s \approx 10^{12}\,\mathrm{Hz},~\omega \sim 30\cdot 10^{12}\,\mathrm{s}^{-1},~\mathrm{permeability}$ of the metal at the high frequencies $\mu \approx 10^4\,\mathrm{G/Oe},~\mathrm{the}$ refractive index $n_0 \approx 10,~(n_\uparrow - n_\downarrow) \approx P(n_\uparrow + n_\downarrow),~(n_\uparrow + n_\downarrow) \approx 10^{22}\,\mathrm{cm}^{-3},$ the polarization degree $P\approx 0.1.$ We also use the estimate $\partial I/\partial p \approx I/p_0~(p_0 = \hbar/a \approx 10^{-19}\,\mathrm{erg\cdot s/cm})$ and that $N_p = 1$ (spontaneous radiation). For these values $R_{st} \approx 10^{17}\ldots 10^{18}\,\mathrm{s}^{-1}\cdot\mathrm{cm}^3$ and $W\approx 10^{-5}-10^{-4}\,\mathrm{W},~\mathrm{which}$ approximately correspond to the experimental range with correction for decay in the metal thickness.

The electron transiting the boundary between the layers changes its energy due to change of exchange energy, since magnetization of the medium varies from \mathbf{M}_1 to \mathbf{M}_2 (the transverse component of the spin to magnetization

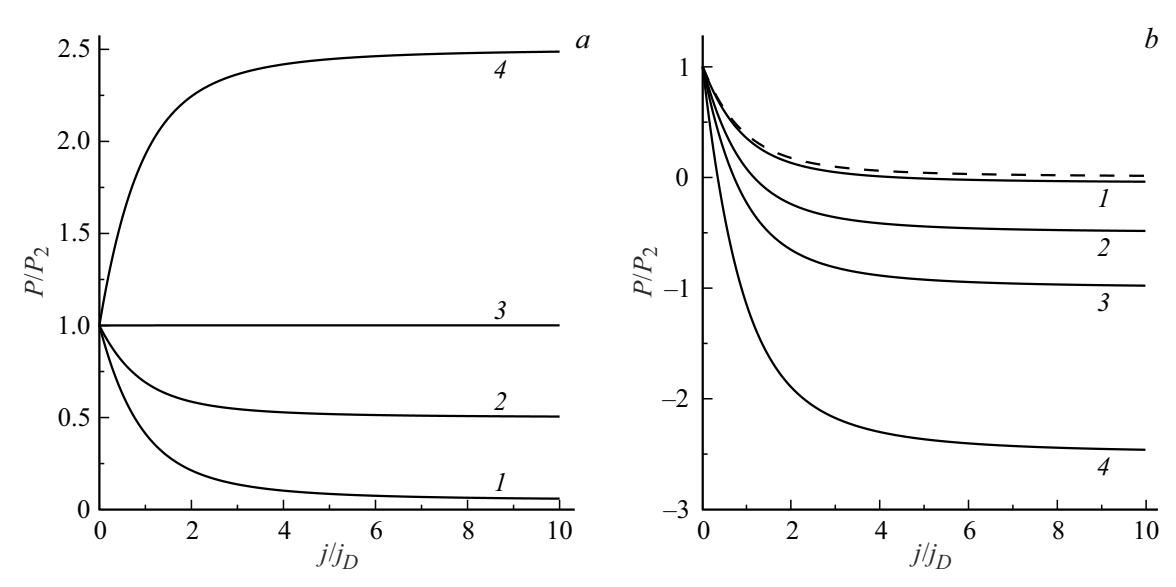


Figure 5. Spin polarization at the boundary of the two ferromagnetics (as related to the equilibrium value) depending on (dimensionless) current density j/j_D with $\varphi = 60^\circ$ (a) and 120° (b) and with different values of a polarization ratio $P_1/P_2 = 0.1$ (1), 1 (2), 2 (3), 5 (4). The dashed line, $P_1/P_2 = 5$, $\varphi = 90^\circ$.

 \mathbf{M}_2 relaxes quite quickly in a time scale of longitudinal relaxation, which we consider here [20–22]). At the same time, the electron which had an antiparallel direction of the spin in relation to \mathbf{M}_1 , gets parallel orientation of the spin in relation to magnetization \mathbf{M}_2 . Thus, it losses a portion of the energy transiting to the lower energy level in relation to the Fermi equilibrium level. And vice versa, the electron with the opposite direction gains energy. An additional expansion in antiparallel orientation of magnetizations (along the quantization axis z) of the quasilevels to the expansions (1), (2), related to this process, can be evaluated by the formula:

$$\Delta \varepsilon_{F-,+} = |\alpha_{sd}\mu_B M_1 - \alpha_{sd}\mu_B M_2| = \alpha_{sd}\mu_B |\Delta M|. \tag{9}$$

Thus, taking into account the formulas (2), (3), (9), the frequency of dynamic radiation $\omega \approx \Delta \varepsilon / \hbar$ caused by energy variation when transiting the interface of the two layers can be written as follows

$$\omega = \frac{2\alpha_{sd}\mu_B\Delta M}{\pi h} + \frac{\hbar(3\pi^2 n)^{2/3}}{4\pi m} \left(\left| \left(\frac{1 - P_2 - \Delta P}{2} \right)^{2/3} - \left(\frac{1 - P_2}{2} \right)^{2/3} \right| + \left| \left(\frac{1 + P_2}{2} \right)^{2/3} - \left(\frac{1 + P_2 + \Delta P}{2} \right)^{2/3} \right| \right).$$
(10)

In accordance with the formula (10), the radiation frequency has two components which are formed by a respective mechanism. As per the first summand (see the formula (9)), reduction of the electron energy with transition to the lower energy levels in one subband can result in radiation of the energy quantum $\Delta \varepsilon_{F-}$ without alteration of spin orientation, i.e. without imposing any additional conditions just after intersecting the layer interface. As the current increases, this radiation becomes noticeable, when

the number of emitted quanta exceeds the number of quanta absorbed by the medium [2]. This process is characterized by a smooth nature of power increase with growth of the current. Let us evaluate the energy slit $\Delta \varepsilon_{\rm F-}$, by assuming the values $\alpha_{sd} = 2 \cdot 10^4$, $\mu_B = 9.3 \cdot 10^{-21}$ erg/G, $\Delta M \sim 10^3$ G. It gives $\Delta \varepsilon \sim 2 \cdot 10^{-20}$, which corresponds to the frequency $\omega \sim 30 \, {\rm s}^{-1}$.

At the same time, the electron gaining antiparallel orientation of the spin in relation to M_2 , increases its energy by the power supply, transiting to the higher energy level in relation to the Fermi equilibrium level. Since the energy changes faster than the spin state, then, as noted above, each of the subbands has the Fermi quasi-levels formed. The energy slit between them is determined by the second term of (10), which corresponds to maximum energy of the electron in the radiative transition. Its quantitative estimate at P = 0.4 gives the value $\Delta \varepsilon = 8.8 \cdot 10^{-20}$, which in terms of an order of magnitude corresponds to the slit with variation of sd-exchange interaction. But in this case, according to [12–14], the radiative transitions are possible with creation of inverse population of the spin subbands. Actually, the spin-polarized electrons go from the injector into the operating region which is already occupied by the spin-polarized electrons. As a result, the equilibrium spin polarization in the operating layer is disturbed. However, emergence of radiation requires creation of conditions, when the concentration of the "hot" electrons in the subband with antiparallel orientation of the spins would exceed the concentration in the opposite subband. According to [17], the inverse population of the spin subbands is determined by the density of current penetrating the magnetic junction. The estimate of this process taken from [17] is plotted on Fig. 5 (calculation by the formula (1)).

As it is clear from Fig. 5, the inverse population corresponding to negative values of polarization of the injected electrons P emerges only with equilibrium spin polarization P>0 and with reaching certain current densities. Thus, the curve P corresponds to the case Fe/Fe, while the curve P is closer to the case Fe₃O₄/Fe. These result demonstrate that the interband radiative transitions appear only when a certain current value is exceeded, i.e. when the process is of a threshold nature.

Thus, a complex mechanism of spin-injected excitation of radiation is shown. Thus, with increase of the current density from zero, starting from a certain, starting value we observe smooth increase of the power due to variation of the energy of *sd*-exchange without alteration of spin orientation. With further increase of the current density, transiting the certain threshold value (which depends on the used ferromagnetic), there is radiation due to the interband transitions with spin flip. The threshold nature of this radiation results in the power jump on the curve of power dependence on the current density.

Conclusion

The double mechanism of THz-radiation excitation when the current flows through the magnetic nanojunction is experimentally established. The radiation excitation is observed both due to variation of the energy of *sd*-exchange when intersecting the interface of the layers with different parameters of the magnetic field without alteration of spin orientation as well as to the interband radiative transitions under effect of external radiation with alteration of spin orientation in some electrons in the energy-excited state. The presence of the certain "dip" of the power before its jump indicates possible phonon absorption during emergence of radiation related to the indirect quantum transitions.

Funding

This study has been carried out under the sate assignment of the Kotelnikov Institute of Radio Engineering and Electronics of the RAS No FFWZ-2022-0016.

Conflict of interest

The authors declare that they have no conflict of interest.

References

 S.S. Dhillon, M.S. Vitiell, E.H. Linfield, A.G. Davies, M.C. Hoffmann, J. Booske, C. Paoloni, M. Gensch, P. Weightman, G.P. Williams, E. Castro-Camus, D.R.S. Cumming, F. Simoens, I. Escorcia-Carranza, J. Grant, S. Lucyszyn, M. Kuwata-Gonokami, K. Konishi, M. Koch, C.A. Schmuttenmaer, T.L. Cocker, R. Huber, A.G. Markelz, Z.D. Taylor, V.P. Wallace, J.A. Zeitler, J. Sibik, T.M. Korter, B. Ellison, S. Rea, P. Goldsmith, K.B. Cooper, R. Appleby, D. Pardo,

- P.G. Huggard, V. Krozer, H. Shams, M. Fice, C. Renaud, A. Seeds, A. Stohr, M. Naftaly, N. Ridler, R. Clarke, J.E. Cunningham, M.B. Johnston. J. Phys. D: Appl. Phys., **50** (4), 043001 (2017). DOI: 10.1088/1361-6463/50/4/043001
- Yu.V. Gulyaev, P.E. Zil'berman, S.G. Chigarev. J. Commun. Technol. Electron., 60 (5), 411 (2015).
 DOI: 10.1134/S1064226915050058
- [3] Yu.V. Gulyaev, P.E. Zil'berman, E.M. Epshtein, R.J. Elliot. J. Commun. Technol. Electron., 48 (9), 942 (2003).
- [4] A. Kadigrobov, R.I. Shekhter, M. Jonson. Low Temp. Phys., 31 (4), 352 (2005). DOI: 10.1063/1.1884439
- Yu.V. Gulyaev, P.E. Zilberman, I.V. Malikov, G.M. Mikhailov,
 A.I. Panas, S.G. Chigarev, E.M. Epshtein. JETP Lett., 93 (5),
 259 (2011). DOI: 10.1134/s0021364011050055
- P. Stremoukhov, A. Safin, M. Logunov, S. Nikitov, A. Kirilyuk.
 J. Appl. Phys., 125 (15), 223903 (2019).
 DOI: 10.1063/1.5090455
- A.M. Kadigrobov, R.I. Shekhter, S.I. Kulinich, M. Jonson,
 O.P. Balkashin, V.V. Fisun, Yu.G. Naidyuk, I.K. Yanson,
 S. Andersson, V. Korenivski. New J. Phys., 13 (2), 023007 (2011). DOI: 10.1088/1367-2630/13/2/023007
- [8] A.M. Kadigrobov, R.I. Shekhter, M. Jonson. Low Temp. Phys., 38 (12), 1439 (2012). DOI: 10.1063/1.4770510
- [9] V. Korenivski, A. Iovan, A. Kadigrobov, R.I. Shekhter. Europhys. Lett., 104 (2), 27011 (2013). DOI: 10.1209/0295-5075/104/27011
- [10] S.G. Chigarev, L.A. Fomin, D.P. Rai, E.A. Vilkov, O.A. Byshevsky-Konopko, D.L. Zagorsky, I.M. Doludenko, A.I. Panas. SPIN, 13 (1), 2350010 (2023). DOI: 10.1142/S2010324723500108
- [11] L.A. Fomin, A.V. Chernykh, V.A. Berezin, E.A. Vilkov. J. Surf. Investig., 15 (1), 128 (2021).
 DOI: 10.1134/S1027451021010237
- [12] A.M. Kadigrobov, Z. Ivanov, T. Claeson, R.I. Shekhter,
 M. Jonson. Europhys. Lett., 67 (6), 948 (2004).
 DOI: 10.1209/epl/i2004-10159-8
- [13] Yu.V. Gulyaev, P.E. Zil'berman, E.M. Epshtein. J. Commun. Technol. Electron., 57 (5), 506 (2012).
 DOI: 10.1134/S106422691205004X
- [14] Yu.V. Gulyaev, P.E. Zil'berman, A.I. Krikunov, A.I. Panas, E.M. Ephshtein. Jetp Lett., 85 (3), 160 (2007). DOI: 10.1134/S002136400703006X
- [15] Yu.V. Gulyaev, E.A. Vilkov, S.G. Chigarev, R.S. Kulikov, A.R. Safin, N.N. Udalov, R.S. Davydenko, A.G. Kolesnikov, A.V. Ognev, G.M. Mikhailov, A.V. Chernykh, S.V. Il'in. J. Commun. Technol. Electron., 63 (8), 928 (2018). DOI: 10.1134/S1064226918080065
- [16] Yu.V. Gulyaev, P.E. Zilberman, A.I. Panas, E.M. Epshtein. Phys.-Usp., **52** (4), 335 (2009).
 DOI: 10.3367/UFNe.0179.200904b.0359
- [17] E.A. Vilkov, G.M. Mikhailov, S.G. Chigarev, Yu.V. Gulyaev, V.N. Korenivskii, S.A. Nikitov, A.N. Slavin. J. Commun. Technol. Electron., 61 (9), 995 (2016). DOI: 10.1134/S1064226916090138
- [18] L.D. Landau, E.M. Lifshitz. *Kvantovaya mekhanika*. *Nerely-ativistkaya teoriya* (Nauka, M., 1974) (in Russian).
- [19] Yu.V. Gulyaev, E.A. Vilkov, P.E. Zilberman, G.M. Mikhailov, S.G. Chigarev. J. Commun. Technol. Electron., 58 (12), 1137 (2013). DOI: 10.1134/S1064226913110077

- [20] E.A. Vilkov, G.M. Mikhailov, S.A. Nikitov, A.R. Safin,
 M.V. Logunov, V.N. Korenivskii, S.G. Chigarev, L.A. Fomin.
 Phys. Solid State, 61 (6), 941 (2019).
 DOI: 10.1134/S1063783419060283
- [21] J.C. Slonczewski. J. Magn. Magn. Mater., **159** (1–2), L1 (1996). DOI: 10.1016/0304-8853(96)00062-5
- [22] L. Berger. Phys. Rev. B, 54 (13), 9353 (1996).DOI: 10.1103/PhysRevB.54.9353

Translated by M.Shevelev